J Mater Sci: Mater Med (2010) 21:439–444
DOI 10.1007/s10856-009-3904-0

Apatite-forming ability of Ti–15Zr–4Nb–4Ta alloy induced by calcium solution treatment

Seiji Yamaguchi · Hiroaki Takadama · Tomiharu Matsushita · Takashi Nakamura · Tadashi Kokubo

Received: 25 June 2009 / Accepted: 5 October 2009 / Published online: 20 October 2009

Abstract Ti–15Zr–4Nb–4Ta alloy free from cytotoxic elements shows high mechanical strength and high corrosion resistance. However, simple NaOH and heat treatments cannot induce its ability to form apatite in the body environment. In the present study, this alloy was found to exhibit high apatite-forming ability when it was treated with NaOH and $CaCl_2$ solutions, and then subjected to heat and hot water treatments to form calcium titanate, rutile, and anatase on its surface. Its high apatite-forming ability was maintained even in 95% relative humidity at 80°C after 1 week. The surface layer of the treated alloy had scratch resistance high enough for handling hard surgical devices. Thus, the treated alloy is believed to be useful for orthopedic and dental implants.

1 Introduction

Titanium (Ti) alloys such as Ti–6Al–4V and Ti–6Al–7Nb have been widely used as orthopedic implants because of their high mechanical strengths and good biocompatibilities. Recently, new kinds of titanium-based alloys excluding elements suspected of cytotoxicity, such as vanadium (V) and aluminum (Al) [1–3], are being developed [4–9]. Ti–15Zr–4Nb–4Ta alloy is one such alloy, and it shows high mechanical strength, relatively low elastic modulus, and better corrosion resistance compared with the Ti–6Al–4V alloy [5, 6]. However, this alloy does not bond to living bone.

It has been reported that simple chemical NaOH and heat treatments can provide bone-bonding ability in pure Ti metal [10–12] and its alloys such as Ti–6Al–4V, Ti–15Mo–5Zr–3Al, and Ti–6Al–2Nb–1Ta [13–15]. Because of their convenience and effectiveness, these kinds of chemical and heat treatments were applied to a porous Ti surface layer of an artificial total hip joint made of a Ti–6Al–2Nb–1Ta alloy. This bioactive artificial hip joint has been clinically used in Japan since 2007. However, these treatments are not effective for inducing bioactivity in Ti–15Zr–4Nb–4Ta alloys.

In the present study, chemical and heat treatments effective for inducing bioactivity in Ti–15Zr–4Nb–4Ta alloys were investigated. Bioactivity was evaluated by the apatite-forming ability in a simulated body fluid (SBF) with ion concentrations nearly equal to those of human blood plasma [16, 17].

2 Materials and methods

2.1 Surface treatments

The Ti–15Zr–4Nb–4Ta alloy (Kobe Steel, Ltd., Ti: Bal., Zr: 14.51, Nb: 3.83, Ta: 3.94, Pd: 0.16, O: 0.25 mass%) was cut into rectangular plates 10 × 10 × 1 mm^3 in size, abraded with #400 diamond plates, and washed with acetone, 2-propanol, and ultrapure water in an ultrasonic cleaner for 30 min each, and dried at 40°C. The alloy samples were soaked in 5 ml of a 5 M NaOH aqueous solution at 60°C for 24 h. After removal from the solution,

S. Yamaguchi (✉) · H. Takadama · T. Matsushita · T. Kokubo
Department of Biomedical Sciences, College of Life and Health Sciences, Chubu University, 1200 Matsumoto-cho, Kasugai-city, Aichi 487-8501, Japan
e-mail: sy-esi@isc.chubu.ac.jp

T. Nakamura
Department of Orthopaedic Surgery, Graduate School of Medicine, Kyoto University, Kawaharacho 54, Shogoin, Sakyo-ku, Kyoto 606-8507, Japan

they were gently rinsed with ultrapure water for 30 s and dried at 40°C. The treated alloy samples were subsequently soaked in 10 ml of 100 mM $CaCl_2$ solution at 40°C for 24 h, and washed and dried in a similar manner. Then, they were heated to 600°C at a rate of 5°C/min and kept for 1 h, followed by natural cooling in an electrical furnace. After the heat treatment, they were soaked in 10 ml of ultrapure water at 80°C for 24 h, and then washed and dried.

2.2 Surface analyses

The surfaces of the alloy samples subjected to the chemical and heat treatments were analyzed by field emission scanning electron microscopy (FE-SEM: S-4300, Hitachi Co., Tokyo, Japan) equipped with energy dispersive X-ray (EDX: EMAX-7000, HORIBA Ltd., Kyoto, Japan) spectroscopy, Auger electron spectroscopy (AES: PHI-670, ULVAC-PHI Inc., Kanagawa, Japan), thin-film X-ray diffractometry (TF-XRD: RINT-2500, Rigaku Co., Tokyo, Japan), and Fourier transform confocal laser Raman spectroscopy (FT-Raman: LabRAM HR800, HORIBA Jobin–Yvon, France). In the FE-SEM and EDX analyses, accelerating voltages of 15 and 5 kV, respectively, were selected. In the TF-XRD measurement, a Cu Kα X-ray source was used at 50 kV and 200 mA, with 0.01° step widths, 1 s/step scans, and 1° glancing angles against the incident beam. In the FT-Raman measurements, an argon (Ar) laser with a wavelength of 514.5 nm was used as a laser source.

Cross-sections of the alloy were also observed under FE-SEM with the same conditions as described above.

The scratch resistance of the surface layer formed on the alloy samples by the chemical and heat treatments was measured using a thin-film scratch tester (CSR-2000, Rhesca Co. Ltd., Tokyo, Japan), using a stylus 5 μm in diameter with a spring constant of 200 g/mm. Based on the standard JIS R-3255, the amplitude, scratch speed, and loading rates were 100 μm, 10 μm/s, and 100 mN/min, respectively.

2.3 Apatite formation in SBF

The alloy samples subjected to the chemical and heat treatments were soaked in 24 ml of SBF with ion concentrations (Na^+ 142.0, K^+ 5.0, Ca^{2+} 2.5, Mg^{2+} 1.5, Cl^- 147.8, HCO_3^- 4.2, HPO_4^{2-} 1.0, and SO_4^{2-} 0.5 mM) nearly equal to those of human blood plasma at 36.5°C. The SBF was prepared by dissolving reagent grade NaCl, $NaHCO_3$, KCl, $K_2HPO_4{\cdot}3H_2O$, $MgCl{\cdot}6H_2O$, $CaCl_2$, and Na_2SO_4 (Nacalai Tesque Inc., Kyoto, Japan) in ultrapure water, and buffered at pH = 7.4 with tri-hydroxymethylaminomethane $(CH_2OH)_3CNH_2$ and 1 M HCl (Nacalai Tesque Inc., Kyoto, Japan) at 36.5°C [16, 17]. After soaking in SBF for 3 d, the samples were removed, gently rinsed with ultrapure water for 30 s, and dried at 40°C. Apatite formation on their surfaces was examined by TF-XRD, FE-SEM, and EDX. To examine the stability of the apatite-forming ability, the treated alloy samples were kept for one week in an incubator with a relative humidity of 95% at 80°C. After removal from the incubator, their apatite-forming abilities were examined by soaking in SBF for 3 d.

3 Results

3.1 Surface structures

Table 1 shows the EDX results for the surfaces of the untreated alloy samples and those subjected to the NaOH, $CaCl_2$, heat, and water treatments. The table shows that about 3.8 at.% of sodium (Na) was incorporated into the surface of the alloy. By the second $CaCl_2$ treatment, the incorporated Na was completely replaced with calcium (Ca), and a little more Ca was incorporated into the surface. The amount of the incorporated Ca was not changed by the heat treatment, but was decreased a little by the final water treatment.

Figure 1 shows an AES depth profile of the surface of the Ti–15Zr–4Nb–4Ta alloy subjected to the NaOH, $CaCl_2$, heat, and water treatments. The figure shows that zirconium

Table 1 Chemical compositions of surface layers of Ti–15Zr–4Ta–4Nb alloy untreated and subjected to NaOH, $CaCl_2$, heat and water treatments, which were analyzed by EDX

	Elements (at.%)							
	O	Ti	Na	Ca	Zr	Nb	Ta	Pd
Untreated	7.2	82.8	0	0	7.1	2.0	0.7	0.1
NaOH	58.1	36.2	3.8	0	1.0	0.6	0.2	0.0
NaOH–$CaCl_2$	58.4	34.5	0	5.6	0.8	0.5	0.3	0.1
NaOH–$CaCl_2$–heat	58.2	34.9	0	5.4	0.7	0.5	0.2	0.0
NaOH–$CaCl_2$–heat–water	58.6	35.6	0	4.4	0.7	0.5	0.2	0.0

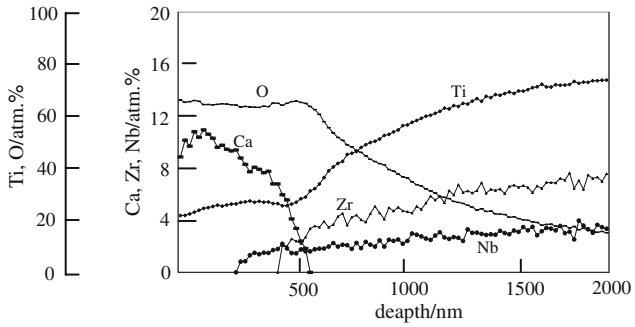

Fig. 1 AES depth profiles of the surface of Ti–15Zr–4Nb–4Ta alloy subjected to NaOH, $CaCl_2$, heat and water treatments

(Zr) and niobium (Nb) were completely removed from the surface layer to a depth of 250 nm and that Ca and oxygen (O_2) penetrated into the surface layer to depths of 500 nm and 1500 nm, respectively. Both of them showed a gradual decrease with increasing depth. Note that the Ca content is slightly decreased at the top surface.

Figure 2 shows FE-SEM photographs of the surfaces of the Ti–15Zr–4Nb–4Ta alloy subjected to the NaOH, $CaCl_2$, heat, and water treatments compared with the untreated alloy. A fine network structure was formed on the nanometer scale by the first NaOH treatment; it was essentially unchanged by the subsequent $CaCl_2$ and heat treatments, but slightly modified with small particles after the final water treatment.

Cross-sectional FE-SEM photographs of these alloy samples are shown in Fig. 3. It can be seen that the fine network structure formed by the first NaOH treatment consists of featherlike phases about 500 nm in length, elongated perpendicular to the surface. The density of the surface layer increased with increasing depth. Its structure was essentially unchanged by the subsequent $CaCl_2$, heat, and water treatments.

Figure 4 shows TF-XRD and FT-Raman profiles of the surface of the untreated alloy samples and those subjected to the NaOH, $CaCl_2$, heat, and water treatments. Broad, small peaks attributed to sodium hydrogen titanate, $Na_xH_{2-x}Ti_3O_7$ [18, 19], appeared after the first NaOH treatment. They were almost unchanged even after the second $CaCl_2$ treatment, indicating that the sodium hydrogen titanate on the surface was isomorphously transformed into calcium hydrogen titanate, $Ca_xH_{2-2x}Ti_3O_7$, by substituting Na in the sodium hydrogen titanate with Ca. The calcium hydrogen titanate was dehydrated to transform into calcium titanate whose phases were assumed to be $CaTi_4O_9$ and $CaTi_2O_4$ [20, 21], and rutile by the subsequent heat treatment. Thus, the formed calcium titanate remained even after the final water treatment, accompanied by small amounts of newly formed anatase. All of these phases are considered to occur at nanometer sizes from their broad X-ray diffraction peaks.

The scratch resistance of the surface of the Ti–15Zr–4Nb–4Ta alloy was as low as 10 mN after the first NaOH and second $CaCl_2$ treatments. This remarkably increased up to about 170 mN after the heat treatment and did not decrease even after the final water treatment.

3.2 Apatite formation

Figure 5 shows FE-SEM photographs of the surfaces of the alloy samples that were soaked in SBF for 3 d after the NaOH, $CaCl_2$, heat, and water treatments. The figure shows that some spherical precipitates were formed on the NaOH-treated alloy. These spherical precipitates increased slightly after the second $CaCl_2$ treatment, but were lost with the heat treatment. After the final water treatment, they remarkably increased to cover the whole surface within 3 d in SBF. These spherical precipitates were identified as crystalline

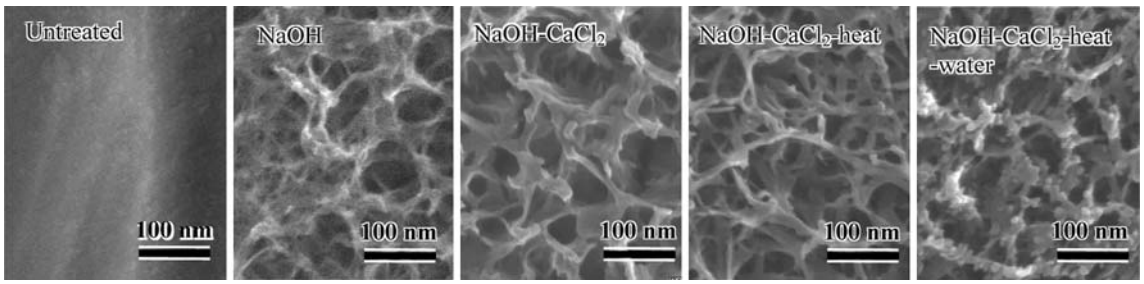

Fig. 2 FE-SEM photographs of the surfaces of Ti–15Zr–4Nb–4Ta alloy after NaOH, $CaCl_2$, heat and water treatments in comparison with that of untreated alloy

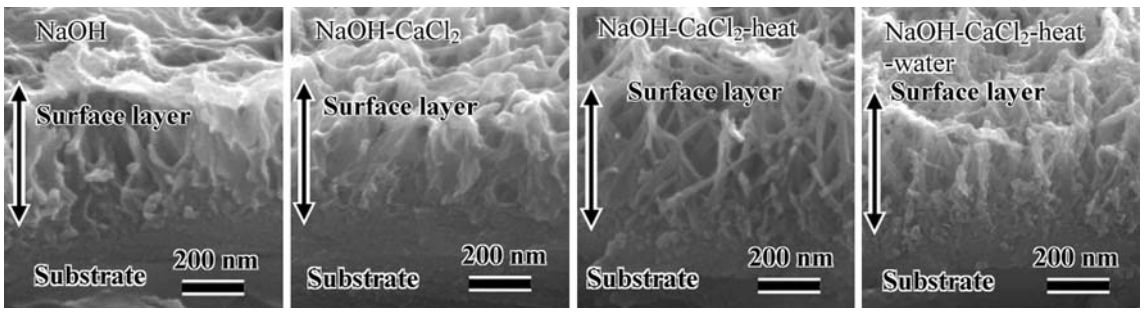

Fig. 3 FE-SEM photographs of the cross-sections of Ti–15Zr–4Nb–4Ta alloy after NaOH, $CaCl_2$, heat and water treatments

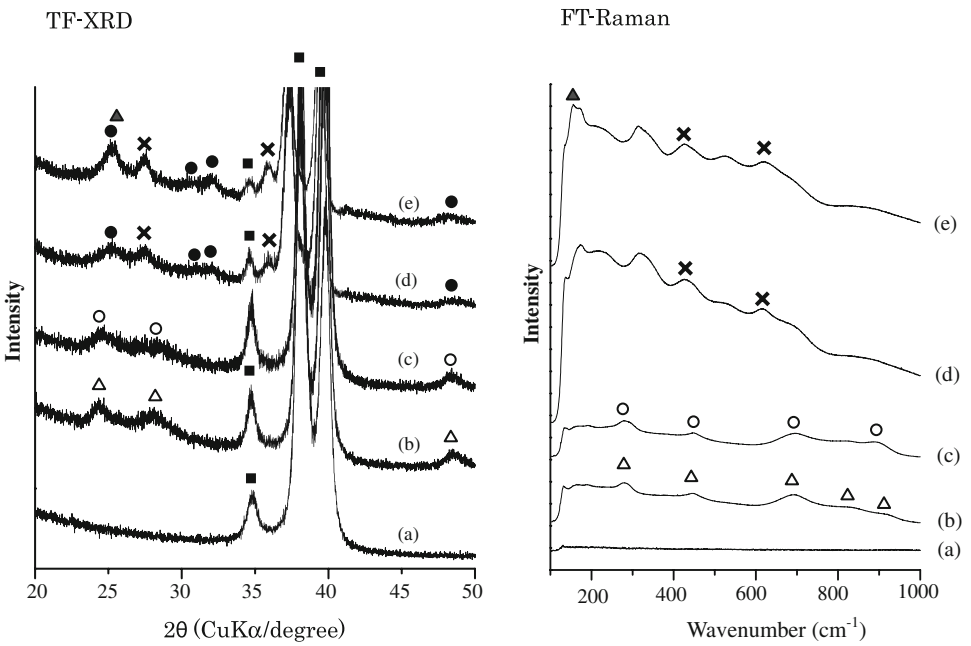

Fig. 4 TF-XRD and FT-Raman profiles of the surfaces of Ti–15Zr–4Ta–4Nb alloy (a) before and after (b) NaOH treatment, (c) NaOH and $CaCl_2$ treatments, (d) NaOH, $CaCl_2$ and heat treatments and (e) NaOH, $CaCl_2$, heat and water treatments. (■) α-Titanium; (△) Sodium hydrogen titanate ($Na_xH_{2-x}Ti_3O_7$); (○) Calcium hydrogen titanate ($Ca_xH_{2-2x}Ti_3O_7$); (●) Calcium titanate ($CaTi_4O_9$, $CaTi_4O_9$); (×) Rutile; (▲) Anatase

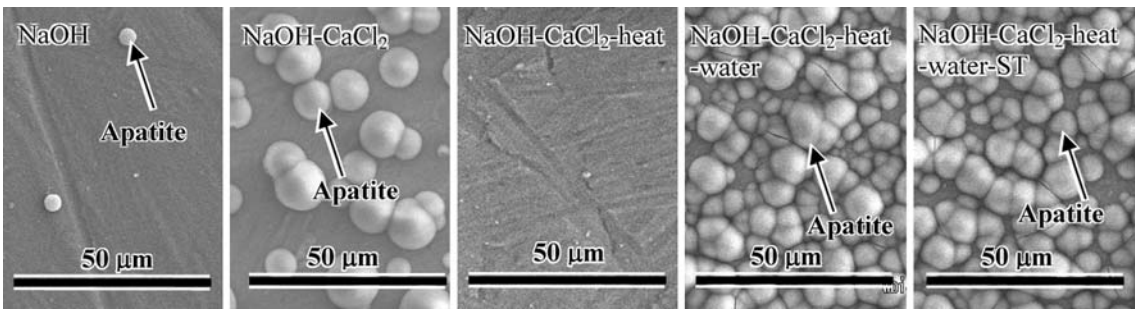

Fig. 5 FE-SEM photographs of the surfaces of Ti–15Zr–4Ta–4Nb alloy that were soaked in SBF for 3 days after NaOH, $CaCl_2$, heat and water treatments, and after subsequent stability test (ST) in humid environment

apatite by TF-XRD. The high apatite-forming ability was maintained even after the stability test in a humid environment.

4 Discussion

Structural changes of the surface of the Ti–15Zr–4Nb–4Ta alloy because of the NaOH, $CaCl_2$, heat, and water treatments are schematically shown in Fig. 6, based on the experimental results. A brush-like structure about 500 nm in thickness, consisting of featherlike phases elongated perpendicular to the surface, was formed on the surface of the alloy by the NaOH treatment. The featherlike phases consisted of nanosized sodium hydrogen titanate that takes a layered structure [19] and, hence, easily substitutes Ca^{2+} ions for Na^+ ions to form a calcium hydrogen titanate, by the $CaCl_2$ treatment. Thus, the formed calcium hydrogen titanate transformed into calcium titanates such as $CaTi_4O_9$ and $CaTi_2O_4$, and rutile by dehydration on the subsequent heat treatment. The calcium titanates and rutile were mostly unchanged by the water treatment, but a small amount of them transformed into anatase by releasing Ca^{2+} ions. From the experimental results described above, it is apparent that the apatite-forming ability of the Ti–15Zr–4Nb–4Ta alloy is slightly induced in the body environment by the NaOH and $CaCl_2$ treatments. However, the treated alloy has a poor scratch resistance and, hence, is unsuitable for practical applications. It was given high scratch resistance by the subsequent heat treatment but lost its apatite-forming ability. It developed a high scratch resistance and high apatite-forming ability as well as stability in a humid environment after the final water treatment. These variations of the apatite-forming ability of the alloy with the chemical and heat treatments are interpreted in terms of surface structural changes as follows.

Induction of the apatite-forming ability of the alloy by the first NaOH treatment is attributed to the formation

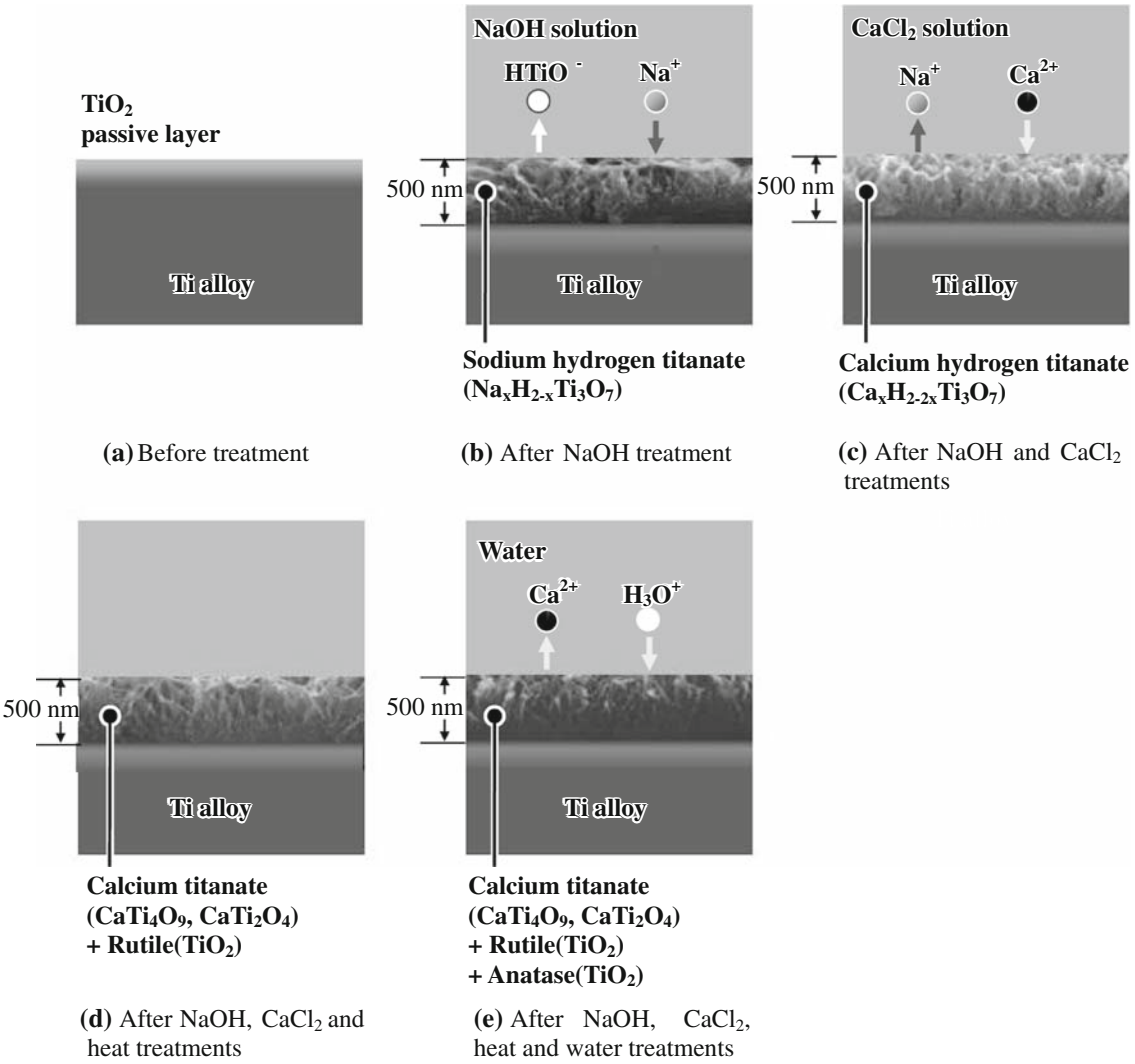

Fig. 6 Schematic illustration of structural changes on the surface of Ti–15Zr–4Nb–4Ta alloy (**a**) by NaOH (**b**), $CaCl_2$ (**c**), heat (**d**) and water (**e**) treatments

of sodium hydrogen titanate on its surface. In SBF, the sodium hydrogen titanate releases its Na^+ ions via exchange with H_3O^+ ions to form Ti–OH groups on its surface. Thus, the formed Ti–OH groups induce apatite formation as earlier described for the NaOH- and heat-treated Ti metal [22–24]. The increased apatite-forming ability of the alloy due to the $CaCl_2$ treatment is attributed to the formation of calcium hydrogen titanate on its surface. The calcium hydrogen titanate more effectively induces apatite formation because the released Ca^{2+} ions increase the ionic activity product of the apatite in the surrounding SBF more effectively than the Na^+ ions do. The loss of the apatite-forming ability of the alloy due to the heat treatment is attributed to the reduced mobility of the Ca^{2+} ions in calcium titanate. The remarkable increase of the apatite-forming ability of the alloy due to the subsequent water treatment is a result of the increased mobility of the Ca^{2+} ions in the calcium titanate by incorporation of H_3O^+ ions during the water treatment. The incorporation of H_3O^+ ions at the surface of the alloy subjected to the water treatment is proved by the decrease in Ca content at its top surface, observed by AES in Fig. 1. The mobility of the Ca^{2+} ions in the calcium titanate is, however, not so high that the Ca content is appreciably decreased in a humid environment. As a result, the high apatite-forming ability of the alloy can be maintained even in 95% relative humidity at 80°C for at least 1 week.

Generally, the mechanical properties of Ti-based alloys are liable to be changed by heat treatment. It is reported, however, that the tensile strength, proof strength, and ductility (reduction in area and elongation) of Ti–15Zr–4Nb–4Ta alloys are hardly affected by heat treatment below 775°C for 1 h [6]. Therefore, heat treatment at 600°C after the NaOH and $CaCl_2$ treatments, which was

used in the present study, does not have an adverse affect on the mechanical strength of the present alloy.

Thus, the treated alloy is expected to form bone-like apatite on its surface, even in the living body, and bond to living bone.

5 Conclusion

Ti–15Zr–4Nb–4Ta alloy, which is free from cytotoxic elements and shows high mechanical strength, can be given a high apatite-forming ability, which is maintained even in a humid environment, and scratch resistance by NaOH, $CaCl_2$, heat, and water treatments. It is believed that this bioactive alloy will be useful in implants in the orthopedic and dental fields in the next generation.

Acknowledgements This work was supported by Translational Research Promotion Project in Health Assurance Program entrusted from the New Energy and Indusrial Techology Development Organization (NEDO). We thank Dr. Yoshimitsu Okazaki for the supply of the alloy.

References

1. Waters MD, Gardner DE, Coffin DL. Cytotoxic effects of vanadium on rabbit alveolar macrophages in vitro. Toxicol Appl Pharmacol. 1974;28:253–63.
2. Steinemann SG. In: Winter GD, Leray JL, de Goot K, editors. Evaluation of biomaterials. New York: Wiley; 1980. p. 1–34.
3. Kawahara H, Ochi S, Tanetani K, Kato K, Isogai M, Mizuno H, et al. Biological testing of dental materials. J Jpn Soc Dent Apparatus Mater. 1963;4:65–75.
4. Maehara K, Doi K, Matsushita T, Sasaki Y. Application of vanadium-free titanium alloys to artificial hip joints. Mater Trans. 2002;43:2936–42.
5. Okazaki Y, Rao S, Ito Y, Tateishi T. Corrosion resistance, mechanical properties, corrosion fatigue strength and cytocompatibility of new Ti alloys without Al and V. Biomaterials. 1998; 19:1197–215.
6. Japanese Industrial Standards. JIST7401-4: titanium materials for surgical implant applications. Part 4. Wrought titanium 15-zirconium 4-niobium 4-tantalum alloy. Tokyo: JISC; 2002.
7. American Society for Testing and Materials. ASTM STP 1272: mechanical and tribological properties and biocompatibility of diffusion hardened Ti–13Nb–13Zr—a new titanium alloy for surgical implants, medical applications of titanium and its alloys: the material and biological issues. Philadelphia: ASTM; 1996.
8. American Society for Testing and Materials. ASTM STP 1272: characterization of Ti–15Mo Beta titanium alloy for orthopedic implant applications, medical applications of titanium and its alloys: the materials and biological issues. Philadelphia: ASTM; 1996.
9. American Society for Testing and Materials. ASTM STP 1471: super elastic functional β titanium alloy with low Young's modulus for biomedical applications. Philadelphia: ASTM; 2006.
10. Kokubo T, Miyaji F, Min-Kim H, Nakamura T. Spontaneous formation of bone-like apatite layer on chemically treated titanium metal. J Amer Ceram Soc. 1996;79:1127–9.
11. Yan QW, Nakamura T, Kobayashi M, Kokubo T, Kim HM, Miyaji F. Bone-bonding behavior of titanium implants prepared via chemical treatment. In: Kokubo T, Nakamura T, Miyaji F, editors. Bioceramics, vol. 9. London: Elsevier; 1996. p. 305–8.
12. Yan QW, Nakamura T, Kobayashi M, Kim HM, Kokubo T. Bonding of chemically treated titanium implants to bone. J Biomed Mater Res. 1997;37:267–75.
13. Kim HM, Miyaji F, Kokubo T, Nakamura T. Preparation of bioactive Ti and its alloy via simple chemical surface treatment. J Biomed Mater Res. 1996;32:409–17.
14. Kim HM, Takadama H, Kokubo T, Nishiguchi S, Nakamura T. Formation of a bioactive graded surface structure on Ti–15Mo–5Zr–3Al alloy by chemical treatment. Biomaterials. 2000;21: 353–8.
15. Nishiguchi S, Kato H, Fujita H, Kim HM, Miyaji F, Kokubo T, et al. Enhancement of bone-bonding strength of titanium alloy implants by alkali and heat treatments. J Biomed Mater Res. 1999;48:689–96.
16. Kokubo T, Takadama H. How useful is SBF in predicting in vivo bone bioactivity? Biomaterials. 2006;27:2907–15.
17. International Organization for Standardization. ISO 23317:2007: implants for surgery—in vitro evaluation for apatite-forming ability of implant materials. Switzerland: ISO; 2007.
18. Sun X, Li Y. Synthesis and characterization of ion-exchangeable titanate nanotubes. Chem Eur J. 2003;9:2229–38.
19. Morgado E Jr, de Abreu MAS, Pravia ORC, Marinkovic BA, Jardim PM, Rizzo FC, et al. A study on the structure and thermal stability of titanate nanotubes as a function of sodium content. Sol St Sci. 2006;8:888–900.
20. Joint Committee on Powder Diffraction Standards (JCPDS) Powder Diffraction Data File 00-026-0333.
21. Joint Committee on Powder Diffraction Standards (JCPDS) Powder Diffraction Data File 01-072-1134.
22. Takadama H, Kim HM, Kokubo T, Nakamura T. An X-ray photoelectron spectroscopy study of the process of apatite formation on bioactive titanium metal. J Biomed Mater Res. 2001;55: 185–93.
23. Takadama H, Kim HM, Kokubo T, Nakamura T. TEM-EDX study of the mechanism of bonelike apatite formation on bioactive titanium metal in simulated body fluid. J Biomed Mater Res. 2001;57:441–8.
24. Kim HM, Himeno T, Kawashita M, Lee JH, Kokubo T, Nakamura T. Surface potential change in bioactive titanium metal during the process of apatite formation in simulated body fluid. J Biomed Mater Res. 2003;67:1305–9.